Cerebral Venous Reflux and Dilated Basal Ganglia Perivascular Space in Hypertensive Intracerebral Hemorrhage

Hsin-Hsi Tsai,[a,b] Bo-Ching Lee,[c] Ya-Fang Chen,[c] Jiann-Shing Jeng,[b] Li-Kai Tsai[b]

[a]Department of Neurology, National Taiwan University Hospital Bei-Hu Branch, Taipei, Taiwan
[b]Department of Neurology, National Taiwan University Hospital, Taipei, Taiwan
[c]Department of Medical Imaging, National Taiwan University Hospital, Taipei, Taiwan

Background and Purpose Cerebral venous flow alterations potentially contribute to age-related white matter changes, but their role in small vessel disease has not been investigated.

Methods This study included 297 patients with hypertensive intracerebral hemorrhages (ICH) who underwent magnetic resonance imaging. Cerebral venous reflux (CVR) was defined as the presence of abnormal signal intensity in the dural venous sinuses or internal jugular vein on time-of-flight angiography. We investigated the association between CVR, dilated perivascular spaces (PVS), and recurrent stroke risk.

Results CVR was observed in 38 (12.8%) patients. Compared to patients without CVR those with CVR were more likely to have high grade (>20 in the number) dilated PVS in the basal ganglia (60.5% vs. 35.1%; adjusted odds ratio [aOR], 2.64; 95% confidence interval [CI], 1.25 to 5.60; P=0.011) and large PVS (>3 mm in diameter) (50.0% vs. 18.5%; aOR, 3.87; 95% CI, 1.85 to 8.09; P<0.001). During a median follow-up of 18 months, patients with CVR had a higher recurrent stroke rate (13.6%/year vs. 6.2%/year; aOR, 2.53; 95% CI, 1.09 to 5.84; P=0.03) than those without CVR.

Conclusions CVR may contribute to the formation of enlarged PVS and increase the risk of recurrent stroke in patients with hypertensive ICH.

Keywords Cerebral small vessel diseases; Hypertension; Cerebral hemorrhage; Perivascular space; Cerebrovenous reflux

Correspondence: Ya-Fang Chen
Department of Medical Imaging, National Taiwan University Hospital, No. 7, Chung-Shan South Road, Taipei 100, Taiwan
Tel: +886-2-23123456 ext.51623
Fax: +886-2-23224552
E-mail: joannayfc@gmail.com
https://orcid.org/0000-0003-2995-9189

Introduction

Spontaneous intracerebral hemorrhage (ICH) is a devastating form of stroke that refers to cerebral intraparenchymal hemorrhage due to the rupture of damaged small arteries or arterioles. Cerebral small vessel disease (SVD), especially hypertensive SVD, is the most common underlying pathology for ICH.[1] Typical radiological presentations that reflect parenchymal injury of SVD on conventional magnetic resonance imaging (MRI) include cerebral microbleeds, white matter hyperintensities (WMHs), lacunes, and dilated perivascular spaces (PVSs) in the basal ganglia (BG).[2,3] While chronic hypertension, aging, and other vascular risk factors contribute to the development of cerebral arteriosclerotic changes in hypertensive ICH, the underlying pathogenesis is probably multi-faceted and remains poorly understood in many respects.[4] The determinants of disease severity and its long-term outcomes in hypertensive ICH remain largely unexplored.

JoS

Tsai et al.   Cerebral Venous Reflux in ICH

Increased cerebral venous pressure contributes to the development of pathological processes in the brain, including blood-brain barrier disruption, perivascular inflammation, remodeling of cerebral venules, and chronic white matter ischemia.[5] Disturbed cerebral venous circulation can be detected by measuring retrograde flows in the internal jugular vein (IJV), the main cerebral venous outflow tract that drains the cerebral superficial and deep venous systems via transverse and sigmoid sinuses. Previous observations indicate that jugular venous reflux is closely related to WMHs in aging and neurodegenerative disorders,[6,7] suggesting that hemodynamic changes in cerebral venous outflow may play a critical role in cerebral SVD.

Recently, some research has explored the pathology of cerebral veins in SVD using neuroimaging measures to elucidate the role of venous circulation in SVD pathogenesis.[8-12] Shaaban et al.[8] showed that increased venular tortuosity on high-field MRI is an early SVD radiological feature, confirming that SVD is related to cerebral venous morphological change. Further studies have revealed that decreased visible deep medullary veins are associated with different SVD neuroimaging biomarkers and total SVD burden, implicating venous collagenosis as an important process during SVD progression.[9-12] Together these findings suggest that venous flow is likely to be altered in SVD. In line with this hypothesis, studies conducted in patients with heart failure have observed an association between increased systemic venous pressure and the development of WMHs, although the underlying mechanism is probably multifactorial and remains to be elucidated.[5,13] An understanding of cerebral venous outflow alteration and how it affects the characteristics of SVD can provide mechanistic insight into the complex role of cerebral venous hypertension in SVD progression. To our knowledge, no other studies investigating cerebral venous reflux (CVR) in SVD or ICH exist, making the current study a pioneering study examining the effect of venous flow reflux, a surrogate marker for increased cerebral venous pressure, in patients with significant arteriosclerosis.

In the present study of spontaneous ICH patients with hypertensive SVD (i.e., cerebral arteriolosclerosis), we first assessed the prevalence of CVR using intracranial magnetic resonance angiography (MRA) to identify the most relevant SVD-related parenchymal injuries during CVR. Second, we aimed to determine the clinical significance of CVR by investigating whether the presence of CVR can predict longitudinal stroke occurrence.

Methods

Data availability

All data from this article are held within the National Taiwan University Hospital (NTUH) and will be shared upon request from a qualified investigator.

Patient enrollment

We included consecutive patients from a prospectively maintained stroke registry consisting of patients with symptomatic ICH treated at NTUH between September 2014 and January 2020 (n=1,450).[14,15] We excluded patients with potential causes of secondary hemorrhage, including trauma, structural and vascular lesions, brain tumors, severe coagulopathy due to systemic disease or medication, or those who had ischemic stroke with hemorrhagic transformation (n=585). Patients who did not undergo a comprehensive MRI study were also excluded (n=486). We categorized each patient into two groups based on their hemorrhagic lesion topography: cerebral amyloid angiopathy (CAA; strictly lobar ICH and microbleeds) or hypertensive ICH (strictly deep or mixed deep and lobar ICH and microbleeds), as previously described.[16] The pons was considered a deep location, while cerebellar hemorrhagic lesions were ignored during categorization because of the unclear nature of underlying cerebral SVD. A total of 297 patients with hypertensive ICH were included in the analysis (Figure 1). Baseline clinical data were systematically collected through a standardized review of medical records. The following clinical variables were recorded for each study subject: age, sex, smoking history, presence or absence of chronic hypertension, classes of antihypertensive medication taken, diabetes mellitus, hypercholesterolemia, atrial fibrillation, and creatinine clearance values (represented by estimated glomerular filtration rate). As we have previously described, follow-up outcome data were collected for research purposes from a systematic review of multiple sources including medical documentation of any clinical visits, imaging databases at NTUH, and phone calls.[14] Patients were followed from their date of enrollment (ICH onset) until the occurrence of death, the last phone call, or the last clinic visit for ICH. Patients who could not be contacted were censored at the time of their last clinic visit, and event occurrence was determined through a comprehensive review of medical records. The occurrence of recurrent symptomatic ICH, incident symptomatic ischemic stroke, and occurrence and cause of death were recorded.
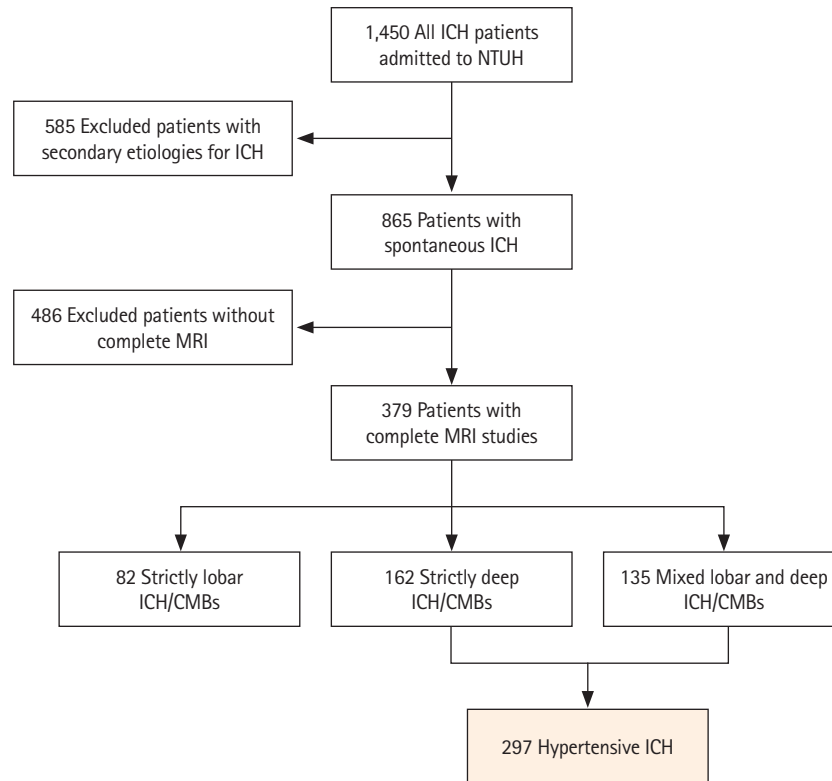
Figure 1. Flowchart of patient enrolment. ICH, intracerebral hemorrhage; NTUH, National Taiwan University Hospital; MRI, magnetic resonance imaging; CMB, cerebral microbleed.

## Standard protocol approvals, registrations, and patient consents

This study was approved by the Institutional Review Board (201903069RINB) of NTUH and is in accordance with their guidelines. Written informed consent was obtained from all participants or their family members.

Image acquisition and analysis

MRIs were performed using a 1.5T (n=114) or 3T (n=183) MRI scanner (MAGNETOM Aera, MAGNETOM Verio, TIM, or Biograph mMR, Siemens Medical Solutions, Malvern, PA, USA) with T1-weighted, T2-weighted, and diffusion-weighted imaging, apparent diffusion coefficient maps, fluid-attenuated inversion recovery (FLAIR) imaging, intracranial time of flight (TOF) angiography, and susceptibility-weighted imaging (SWI). Intracranial TOF MRA was performed in the axial plane using the following parameters: repetition time (TR) range/echo time (TE) range, 20–25/3–7; flip angle, 18°–25°; field-of-view (FOV), 178×200 mm; matrix, 256×196; slice thickness=0.7–1 mm; and section slices, 140. CVR was evaluated using TOF MRA of the IJV and dural venous sinuses (cavernous, inferior petrosal, sigmoid, or transverse sinus) for each patient. Abnormal venous signal intensities were defined as tubular high signal intensities

in the visualized IJV or dural venous sinuses, as shown in Figure 2. The side (right or left) and location of the abnormal venous signals were recorded. In patients with identified CVR on TOF MRA, we carefully examined the presence of abnormal dots of arterial signal on the wall of the dural sinuses or asymmetrical dilatation of the external carotid artery branches to exclude dural arteriovenous fistula. For cases with available contrast-enhanced MRA or computed tomography angiography (n=22), the absence of arteriovenous fistula was reassured.[17-19] Two trained investigators (authors B.C.L. and Y.F.C.), board-certified neuroradiologists who were blinded to the clinical characteristics of the study subjects, evaluated the TOF MRA results individually. A consensus rating was achieved after discussion in cases in which individual assessments differed with regard to the presence or absence of CVR. Subtle unsaturated vascular signals were excluded based on the reader's experience and anatomical continuity.

MRI-visible enlarged perivascular spaces (EPVS) were evaluated on T2-weighted imaging and defined as sharply delineated structures measuring <3 mm following the course of perforating or medullary vessels.[20] The number of EPVS were counted in the centrum semiovale and BG on the side of the brain with more severe involvement. The severity of EPVS were rated

JoS

Tsai et al.   Cerebral Venous Reflux in ICH
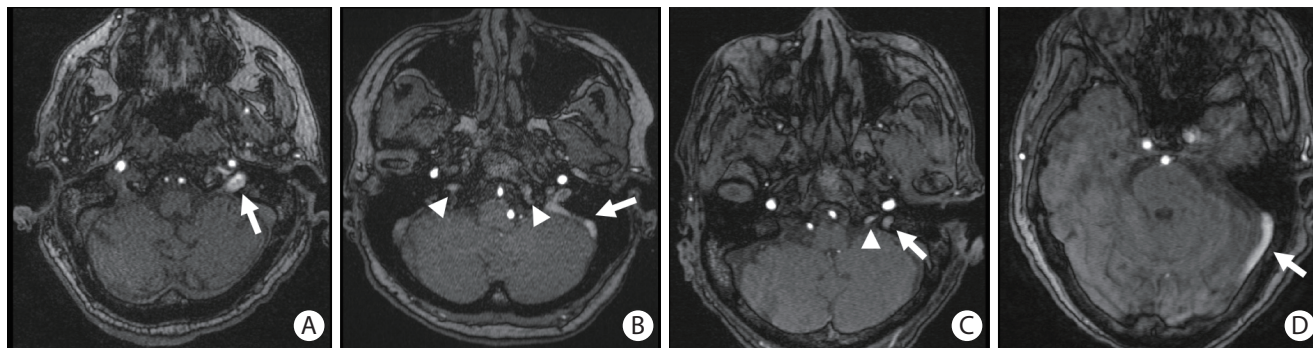
Figure 2. Image of representative cerebral venous reflux (CVR). CVR is detected in (A) the left internal jugular vein (arrow), (B) the left sigmoid sinus (arrow) and bilateral inferior petrosal sinuses (arrowheads), (C) the left internal jugular vein (arrow) and the left inferior petrosal sinus (arrowhead), and (D) the left transverse sinus (arrow).

with a validated 4-point visual scale (0, none; 1, ≤10; 2, 11–20; 3, 21–40; and 4, ≥40).[20,21] According to a previously proposed method, we pre-specified a dichotomized classification of high (scale 3 and 4) or low grade (scale 0 to 2).[20] We also recorded presence or absence of large perivascular spaces (L-PVS) in the BG according to the previously proposed method.[22] L-PVS was defined as round or tubular defects with a short axis larger than 3 mm without a rim or area of high signal intensity on the axial FLAIR MRI or evidence of hemosiderin on the axial SWI.[22] Other MRI markers of cerebral SVD were evaluated as previously described and according to the Standards for Reporting Vascular Changes on Neuroimaging criteria.[3,14] Briefly, the presence and location of cerebral microbleeds were evaluated as previously described.[23] Cerebral microbleeds are defined as lesions with homogeneous round signal loss (less than 10 mm in diameter) on SWI and did not include symmetric hypointensities and flow voids from blood vessels. Cerebral microbleeds were counted in the lobar and deep regions using the Microbleed Anatomical Rating Scale.[24] Lacunes were evaluated in the supratentorial region and defined as "round or ovoid, subcortical, fluid-filled cavity between 3 and 15 mm in diameter."[3,25] WMH volume was calculated based on FLAIR imaging using a semi-automated measure, as previously described.[26,27] Volume estimates were performed in the ICH-free hemisphere of the brain and multiplied by two.

Statistical analysis

We compared the baseline demographic information and neuroimaging variables between patients with and without CVR (Table 1). Discrete variables are presented as counts (%), and continuous variables are presented as mean±standard deviation or median (interquartile range [IQR]), as appropriate, based on their distribution. Categorical variables were analyzed using Fisher's exact test, and continuous variables were analyzed us-

ing an independent-sample t-test (for normal distributions) or Mann-Whitney U test (for non-normal distributions). Univariate and multivariate logistic regression models were built to examine the association between the presence of CVR and dilated PVS (EPVS >20 or L-PVS) in the BG with the covariates of age, sex, and WMH, as shown in Table 2.

The follow-up time for each patient was calculated from the date of ICH until the date of death, last phone interview, or last clinical documentation of ICH. The incidence rate of stroke (defined as the occurrence of ischemic stroke or recurrent ICH) was calculated as the incidence per person-year. Kaplan-Meier analysis was conducted to plot the disease-free probability, and the log-rank test was applied to test the difference between groups. In addition, we built a Cox regression model to calculate the hazard ratio (HR) and 95% confidence interval (CI) for the occurrence of stroke to adjust for age, sex, and other vascular risk factors, including hypertension, diabetes, hyperlipidemia, atrial fibrillation, and smoking history. All statistical analyses were performed using SPSS version 25 (IBM Corp., Armonk, NY, USA). All tests were 2-tailed with a threshold for significance of $P<0.05$.

Results

Among 865 patients with primary ICH, 486 (56.2%) did not undergo brain MRIs (Figure 1). Compared to patients who received MRIs (63.2±13.4 years, male 62.0%), patients without MRIs (61.4±16.6 years, male 65.2%) had higher initial NIH Stroke Scale scores (18.5±11.8 vs. 10.2 vs. 7.7, $P<0.001$), and lower Glasgow Coma Scale scores (11±4 vs. 14±2, $P<0.001$). Of the 297 patients with hypertensive ICH included in the analysis, 38 (12.8%) displayed CVR on MRA. There was no difference in the CVR detection rate between the 1.5T and 3T scanners ($P>0.999$). In patients with CVR, the CVR was located in the

Table 1. Comparison of demographics in patients with and without cerebral venous reflux

Variable	CVR (+) (n=38)	CVR (–) (n=259)	P
Female sex	18 (47.4)	87 (33.6)	0.105
Age (yr)	63.7±12.1	62.6±13.5	0.629
eGFR (mL/min/1.73 m^2)	82.5±29.5	94.3±37.3	0.064
Lobar ICH	6 (15.8)	28 (10.8)	0.410
Hypertension	36 (94.7)	242 (93.4)	>0.999
Diabetes	9 (23.7)	74 (28.6)	0.699
Hyperlipidemia	12 (31.6)	79 (30.5)	>0.999
Atrial fibrillation	4 (10.5)	12 (4.6)	0.133
Smoking history	15 (39.5)	81 (31.3)	0.354
3T MRI scanner	24 (63.2)	159 (61.4)	>0.999
Cerebral microbleed			
Total CMB number	17.3±26.3	8.4±18.2	0.049
Lobar CMB number	9.6±18.0	4.4±12.6	0.093
Deep CMB number	7.7±10.7	4.0±7.1	0.043
Cerebellum CMB number	4.9±12.3	1.7±8.8	0.128
White matter hyperintensity volume (mL)	21.2 (7.4–43.2)	12.4 (6.5–23.0)	0.022
Lacunes (%)	22 (57.9)	109 (42.1)	0.080
Lacune number	1.6±2.3	1.0±1.8	0.087
MRI-visible enlarged PVS			
Centrum semiovale >20	9 (23.7)	68 (26.3)	0.844
Basal ganglia >20	23 (60.5)	91 (35.1)	0.004
Large PVS (>3 mm)	19 (50.0)	48 (18.5)	<0.001

Values are presented as number (%), mean±standard deviation, or median (interquartile range).
CVR, cerebral venous reflux; eGFR, estimated glomerular filtration rate; ICH, intracerebral hemorrhage; MRI, magnetic resonance imaging; CMB, cerebral microbleed; PVS, perivascular space.

Table 2. Univariate and multivariate models in predicting dilated perivascular spaces in patients with hypertensive intracerebral hemorrhage

Variable	OR (95% CI)	P
BG-EPVS >20		
CVR (model 1: univariate)	2.83 (1.41–5.69)	0.004
CVR (model 2: age, sex)	3.00 (1.44–6.25)	0.003
CVR (model 3: age, sex, WMH)	2.64 (1.25–5.60)	0.011
L-PVS		
CVR (model 1: univariate)	4.40 (2.16–8.93)	<0.001
CVR (model 2: age, sex)	4.46 (2.18–9.12)	<0.001
CVR (model 3: age, sex, WMH)	3.87 (1.85–8.09)	<0.001
BG-EPVS >20 or L-PVS		
CVR (model 1: univariate)	4.85 (2.14–10.98)	<0.001
CVR (model 2: age, sex)	5.14 (2.22–11.90)	<0.001
CVR (model 3: age, sex, WMH)	4.57 (1.95–10.69)	<0.001

OR, odds ratio; CI, confidence interval; BG-EPVS, MRI-visible enlarged perivascular spaces in basal ganglia; CVR, cerebrovenous reflux; WMH, white matter hyperintensity; L-PVS, large perivascular space.

inferior petrosal sinus (n=26, 68.4%), sigmoid sinus (n=20, 52.6%), IJV (n=9, 23.7%), or transverse sinus (n=1, 2.6%). Most patients had unilateral CVR more frequently on the left side (left side, n=25; right side, n=7; bilateral, n=6). Nineteen patients (50.0%) had CVR at multiple locations. The inter-rater agreement for detecting CVR was very good (k=0.89; 95% CI, 0.82 to 0.97). Table 1 shows the univariate comparisons of characteristics between patients with CVR (mean age 63.7±12.1 years, female 47.4%) and patients without CVR (62.6±13.5 years, female 33.6%). A higher prevalence of high-grade (scale 3 and 4) MRI-visible BG-EPVS (60.5 vs. 35.1%, P=0.004) and L-PVS (50.0 vs. 18.5%, P<0.001) was observed in patients with CVR than in those without CVR. Patients with CVR also had more cerebral microbleeds (17.3±26.3 vs. 8.4±18.2, P=0.049) and higher WMH volume (21.2 mL [IQR, 7.4 to 43.2] vs. 12.4 mL [IQR, 6.5 to 23.0], P=0.022) compared to patients without CVR. Table 2 shows the results of the univariate and multivariate logistic regression models that investigated CVR in predicting dilated PVS in the BG. In multivariate analyses, after adjusting for age, sex, and WMH volume, the presence of CVR remained

JoS

Tsai et al.   Cerebral Venous Reflux in ICH
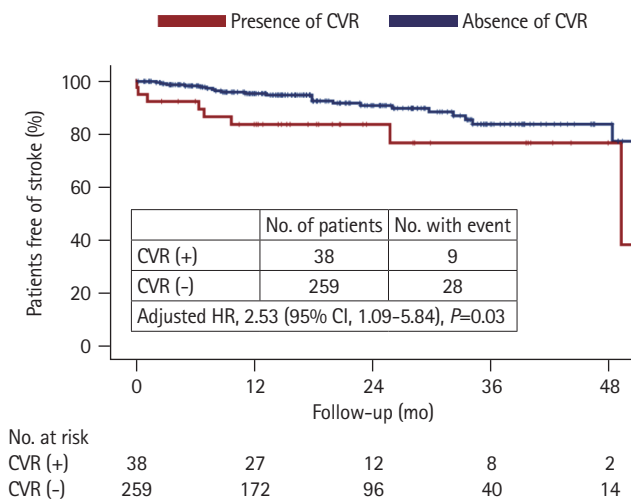
Figure 3. Kaplan-Maier curves for patients with cerebral venous reflux (CVR) and patients without CVR. HR, hazard ratio; CI, confidence interval.

an independent predictor of severe BG-EPVS (odds ratio [OR], 2.64; 95% CI, 1.25 to 5.60; $P=0.011$) or presence of L-PVS (OR, 3.87; 95% CI, 1.85 to 8.09; $P<0.001$).

We further compared the long-term stroke occurrence between patients with and without CVR, with a median follow-up time of 18 months (IQR, 9 to 32). Stroke recurrence was found in nine (23.7%) patients with CVR (three had recurrent ICH, four had incident ischemic stroke, and two had both hemorrhagic and ischemic events) and 28 (10.8%) patients without CVR (19 had recurrent ICH, seven had incident ischemic stroke, and two had both hemorrhagic and ischemic events). Patients with CVR had a higher stroke incidence rate than those without (13.6% per person-year vs. 6.2% per person-year, $P=0.014$) (Figure 3). In the Cox regression model, the presence of CVR predicted a higher risk of stroke occurrence (HR, 2.53; 95% CI, 1.09 to 5.84; $P=0.03$) after adjustment for age, sex, hypertension, diabetes, hyperlipidemia, atrial fibrillation, and smoking history.

Discussion

We detected CVR in 12.8% of the patients with hypertensive ICH using brain MRI with a TOF sequence. CVR was independently associated with dilated PVS in the BG, including a higher prevalence of severe BG-EPVS and L-PVS than in patients without CVR. Our results suggest a close relationship between venous flow alteration and PVS formation in hypertensive SVD patients. Furthermore, in an 18-month follow-up, the presence of CVR was associated with a higher risk of incident stroke, suggesting a detrimental effect of abnormal cerebral venous circulation in survivors of hypertensive ICH. Future in-

vestigations are warranted to delineate the underlying mechanisms of venous flow changes and SVD development.

Presence of CVR is related to the alteration of the venous outflow pathway and possible cerebral venous hypertension.[5] In our study, CVR was more frequently observed on the left side, in keeping with a previous report; authors of that report suggested one possible explanation is that the left IJV is less dominant and thus more predisposed to static or reflux venous flow than the right IJV.[28] Previous studies have identified jugular venous reflux and increased cerebral venous pressure as contributing to the development of WMH in aging and neurodegenerative disorders.[7,29,30] However, research on the venous reflux or venous pressure in SVD is lacking so far. Using a consecutive ICH cohort composed of patients with hypertensive SVD, we identified that 12.8% of the patients had CVR. These patients exhibited more severe SVD radiological markers, particularly profound PVS in deep penetrating vessels. We further found a higher stroke occurrence rate in patients with CVR, supporting the idea that these patients harbor more severe SVD pathology. Our findings indicate that venous outflow alteration and/or venous hypertension are closely related to cerebral SVD and may predispose patients to a higher risk of future stroke events. It remains unclear whether the anatomical location of CVR is associated with its severity and clinical outcomes. Future studies with larger sample sizes and biomarkers for abnormal venous pressure are warranted.

PVS, also called Virchow-Robin spaces, are interstitial fluid-filled spaces around small perforating arteries that can be visible on MRI when they are enlarged.[3,31] In SVD related to chronic hypertension, PVS are frequently visible in the BG, where small vessels tend to be most affected.[22,32] An important finding of this study is the association between cerebral venous flow alteration and an increase in PVS in the BG. Using two different radiological PVS markers (high number of smaller-sized PVS and presence of large-sized PVS), we showed that CVR was significantly related to PVS fluid accumulation around damaged small vessels. In agreement with our findings, terminal venous disruptions were associated with decreased interstitial fluid drainage and MRI-visible PVS in the BG.[33,34] The enlargement of the PVS was associated with dysfunctional brain waste clearance involving the glymphatic system and intramural periarterial drainage pathway.[31,35] Thus, our findings highlight the pathophysiological role of cerebral venous circulation in the effects of perivascular fluid drainage on SVD. This also implies that dysfunctional cerebrospinal fluid and brain fluid dynamics are associated with multifaceted pathologies in the brain and that together these pathologies potentially create a vicious cycle that contributes to SVD progression. Our study

used a cross-sectional design to examine the relationship between CVR and other MRI markers. Future efforts should focus on delineating the causal relationships between disturbed venous flow, PVS fluid accumulation, and SVD progression. The association between CVR and PVS enlargement should also be examined in other SVD populations, such as CAA and in healthy elderly populations. An understanding of venous flow alterations in the pathogenesis of SVD will help identify potential therapeutic targets for treating SVD.

CVR is usually detected by neck ultrasonography showing internal jugular venous reflux spontaneously or during Valsalva maneuvers.[30] In the current study, we used intracranial TOF MRA to detect spontaneous retrograde flows in the dural venous sinuses. TOF-MRA is a common noninvasive technique used to evaluate vascular lesions in the brain. A few radiological reports have used TOF MRA to assess retrograde flow in venous circulation, supporting its feasibility and reproducibility. Similar to what we found in our study, most abnormal signals were present in the inferior petrosal sinus and sigmoid sinus.[19,36-38] Our TOF MRA measure has the advantage of simultaneously examining both bilateral IJVs and other intracranial venous sinuses at the same time. Interestingly, only 23.7% of patients had reflux flow in their IJVs, while the remaining patients had venous flow alterations limited to their intracranial venous sinuses without significant IJV reflux on MRI. Paravertebral venous plexus reflux into dural sinuses or very slow reflux flow in IJV due to large venous caliber can both lead to isolated intracranial venous reflux on MRI.[38] Compared to Doppler ultrasonography, our approach may provide a more sensitive method to detect early or mild CVR that has not yet resulted in terminal outflow alterations.

One major limitation of this study was the determination of CVR using a single MRI. Venous reflux can be a dynamic process in which a provoked response (e.g., during the Vasalva maneuver) or multiple examinations are necessary to detect trivial or transient CVR. Our MRIs was performed in the acute to subacute stages of ICH when patients were receiving guideline-recommended BP control. Therefore, hemodynamic fluctuations may also affect our CVR detection rate; however, this issue is beyond the scope of the current study. Selection bias was also a consideration because those who could not tolerate MRI scans were not included (n=486), such as patients with larger hematoma, hemodynamic instability or early mortality. Another limitation is that we selected patients with hypertensive SVD who experienced symptomatic ICH as our study population. These patients may represent a group with relatively more severe SVD than those presenting with pure lacunar infarct or other clinical manifestations, which will affect the generalizability of our results to the entire SVD population. We also excluded patients with CAA-related ICH to avoid the potential confounding effect of the different topographical distribution of damaged vessels in β-amyloid disorders.[16] Further study focusing on CVR in CAA to delineate the complex relationships between β-amyloid deposition, venous flow alterations and SVD injuries to the brain should be done. Finally, the sample size in this study was relatively small and our cross-sectional design could not assess the causality between CVR and PVS enlargement. Larger studies with longitudinal neuroimaging data are necessary to validate the results presented herein.

Conclusions

In conclusion, abnormal venous flow in patients with hypertensive ICH was significantly associated with a dilated PVS in the BG. The presence of CVR on TOF MRA predicted a higher incidence of future stroke, suggesting a detrimental effect of disturbed venous flow in hypertensive SVD. Our results imply that venous flow alterations are associated with SVD. Further investigations to explore the underlying pathophysiology are warranted to identify potential therapeutic strategies.

Disclosure

The authors have no financial conflicts of interest.

Acknowledgments

References

1. Qureshi AI, Tuhrim S, Broderick JP, Batjer HH, Hondo H, Hanley DF. Spontaneous intracerebral hemorrhage. *N Engl J Med* 2001;344:1450-1460.

2. Tsai HH, Kim JS, Jouvent E, Gurol ME. Updates on prevention of hemorrhagic and lacunar strokes. *J Stroke* 2018;20:167-179.

3. Wardlaw JM, Smith EE, Biessels GJ, Cordonnier C, Fazekas F, Frayne R, et al. Neuroimaging standards for research into small vessel disease and its contribution to ageing and neurodegeneration. *Lancet Neurol* 2013;12:822-838.

JoS

Tsai et al.   Cerebral Venous Reflux in ICH

4. Wardlaw JM, Smith C, Dichgans M. Small vessel disease: mechanisms and clinical implications. *Lancet Neurol* 2019; 18:684-696.

5. Fulop GA, Tarantini S, Yabluchanskiy A, Molnar A, Prodan CI, Kiss T, et al. Role of age-related alterations of the cerebral venous circulation in the pathogenesis of vascular cognitive impairment. *Am J Physiol Heart Circ Physiol* 2019;316:H1124-H1140.

6. Chung CP, Beggs C, Wang PN, Bergsland N, Shepherd S, Cheng CY, et al. Jugular venous reflux and white matter abnormalities in Alzheimer's disease: a pilot study. *J Alzheimers Dis* 2014;39:601-609.

7. Chung CP, Hu HH. Pathogenesis of leukoaraiosis: role of jugular venous reflux. *Med Hypotheses* 2010;75:85-90.

8. Shaaban CE, Aizenstein HJ, Jorgensen DR, MacCloud RL, Meckes NA, Erickson KI, et al. In vivo imaging of venous side cerebral small-vessel disease in older adults: an MRI method at 7T. *AJNR Am J Neuroradiol* 2017;38:1923-1928.

9. Chen X, Wei L, Wang J, Shan Y, Cai W, Men X, et al. Decreased visible deep medullary veins is a novel imaging marker for cerebral small vessel disease. *Neurol Sci* 2020;41: 1497-1506.

10. Zhang R, Li Q, Zhou Y, Yan S, Zhang M, Lou M. The relationship between deep medullary veins score and the severity and distribution of intracranial microbleeds. *Neuroimage Clin* 2019;23:101830.

11. Zhou Y, Li Q, Zhang R, Zhang W, Yan S, Xu J, et al. Role of deep medullary veins in pathogenesis of lacunes: Longitudinal observations from the CIRCLE study. *J Cereb Blood Flow Metab* 2020;40:1797-1805.

12. Xu Z, Li F, Wang B, Xing D, Pei Y, Yang B, et al. New insights in addressing cerebral small vessel disease: association with the deep medullary veins. *Front Aging Neurosci* 2020;12:597799.

13. Alosco ML, Brickman AM, Spitznagel MB, Griffith EY, Narkhede A, Raz N, et al. Independent and interactive effects of blood pressure and cardiac function on brain volume and white matter hyperintensities in heart failure. *J Am Soc Hypertens* 2013;7:336-343.

14. Tsai HH, Chen SJ, Tsai LK, Pasi M, Lo YL, Chen YF, et al. Long-term vascular outcomes in patients with mixed location intracerebral hemorrhage and microbleeds. *Neurology* 2021; 96:e995-e1004.

15. Yeh SJ, Tang SC, Tsai LK, Jeng JS. Pathogenetical subtypes of recurrent intracerebral hemorrhage: designations by SMASH-U classification system. *Stroke* 2014;45:2636-2642.

16. Tsai HH, Pasi M, Tsai LK, Huang CC, Chen YF, Lee BC, et al. Centrum semiovale perivascular space and amyloid deposition in spontaneous intracerebral hemorrhage. *Stroke* 2021;

52:2356-2362.

17. Caton MT, Callen AL, Copelan AZ, Narsinh KH, Smith ER, Amans MR. Jugular venous reflux can mimic posterior fossa dural arteriovenous fistulas on MRI-MRA. *AJR Am J Roentgenol* 2021;216:1626-1633.

18. Lee J, Lee JY, Lee YJ, Park DW, Kim TY, Kim YS, et al. Differentiation of dural arteriovenous fistula from reflux venous flow on 3D TOF-MR angiography: identifying asymmetric enlargement of external carotid artery branches. *Clin Radiol* 2020; 75:714.

19. Kim E, Kim JH, Choi BS, Jung C, Lee DH. MRI and MR angiography findings to differentiate jugular venous reflux from cavernous dural arteriovenous fistula. *AJR Am J Roentgenol* 2014;202:839-846.

20. Charidimou A, Boulouis G, Pasi M, Auriel E, van Etten ES, Haley K, et al. MRI-visible perivascular spaces in cerebral amyloid angiopathy and hypertensive arteriopathy. *Neurology* 2017;88:1157-1164.

21. Doubal FN, MacLullich AM, Ferguson KJ, Dennis MS, Wardlaw JM. Enlarged perivascular spaces on MRI are a feature of cerebral small vessel disease. *Stroke* 2010;41:450-454.

22. Ding J, Sigurðsson S, Jónsson PV, Eiriksdottir G, Charidimou A, Lopez OL, et al. Large perivascular spaces visible on magnetic resonance imaging, cerebral small vessel disease progression, and risk of dementia: the age, gene/environment susceptibility-reykjavik study. *JAMA Neurol* 2017;74:1105-1112.

23. Greenberg SM, Vernooij MW, Cordonnier C, Viswanathan A, Al-Shahi Salman R, Warach S, et al. Cerebral microbleeds: a guide to detection and interpretation. *Lancet Neurol* 2009;8: 165-174.

24. Gregoire SM, Chaudhary UJ, Brown MM, Yousry TA, Kallis C, Jäger HR, et al. The Microbleed Anatomical Rating Scale (MARS): reliability of a tool to map brain microbleeds. *Neurology* 2009;73:1759-1766.

25. Pasi M, Boulouis G, Fotiadis P, Auriel E, Charidimou A, Haley K, et al. Distribution of lacunes in cerebral amyloid angiopathy and hypertensive small vessel disease. *Neurology* 2017; 88:2162-2168.

26. Tsai HH, Pasi M, Tsai LK, Chen YF, Chen YW, Tang SC, et al. Superficial cerebellar microbleeds and cerebral amyloid angiopathy: a magnetic resonance imaging/positron emission tomography study. *Stroke* 2020;51:202-208.

27. Tsai HH, Pasi M, Tsai LK, Chen YF, Lee BC, Tang SC, et al. Microangiopathy underlying mixed-location intracerebral hemorrhages/microbleeds: a PiB-PET study. *Neurology* 2019;92: e774-e781.

28. Lichtenstein D, Saïfi R, Augarde R, Prin S, Schmitt JM, Page

B, et al. The internal jugular veins are asymmetric: usefulness of ultrasound before catheterization. *Intensive Care Med* 2001;27:301-305.

29. Nan D, Cheng Y, Feng L, Zhao M, Ma D, Feng J. Potential mechanism of venous system for leukoaraiosis: from postmortem to in vivo research. *Neurodegener Dis* 2019;19:101-108.

30. Chung CP, Wang PN, Wu YH, Tsao YC, Sheng WY, Lin KN, et al. More severe white matter changes in the elderly with jugular venous reflux. *Ann Neurol* 2011;69:553-559.

31. Wardlaw JM, Benveniste H, Nedergaard M, Zlokovic BV, Mestre H, Lee H, et al. Perivascular spaces in the brain: anatomy, physiology and pathology. *Nat Rev Neurol* 2020;16:137-153.

32. Zhu YC, Tzourio C, Soumaré A, Mazoyer B, Dufouil C, Chabriat H. Severity of dilated Virchow-Robin spaces is associated with age, blood pressure, and MRI markers of small vessel disease: a population-based study. *Stroke* 2010;41:2483-2490.

33. Zhang K, Zhou Y, Zhang W, Li Q, Sun J, Lou M. MRI-visible perivascular spaces in basal ganglia but not centrum semiovale or hippocampus were related to deep medullary veins changes. *J Cereb Blood Flow Metab* 2022;42:136-144.

34. Zhang R, Huang P, Jiaerken Y, Wang S, Hong H, Luo X, et al. Venous disruption affects white matter integrity through increased interstitial fluid in cerebral small vessel disease. *J Cereb Blood Flow Metab* 2021;41:157-165.

35. Gouveia-Freitas K, Bastos-Leite AJ. Perivascular spaces and brain waste clearance systems: relevance for neurodegenerative and cerebrovascular pathology. *Neuroradiology* 2021; 63:1581-1597.

36. Inano S, Itoh D, Takao H, Hayashi N, Mori H, Kunimatsu A, et al. High signal intensity in the dural sinuses on 3D-TOF MR angiography at 3.0 T. *Clin Imaging* 2010;34:332-336.

37. Uchino A, Nomiyama K, Takase Y, Nakazono T, Tominaga Y, Imaizumi T, et al. Retrograde flow in the dural sinuses detected by three-dimensional time-of-flight MR angiography. *Neuroradiology* 2007;49:211-215.

38. Jang J, Kim BS, Kim BY, Choi HS, Jung SL, Ahn KJ, et al. Reflux venous flow in dural sinus and internal jugular vein on 3D time-of-flight MR angiography. *Neuroradiology* 2013;55: 1205-1211.